MEASUREMENTS OF OCTUPOLE COLLECTIVITY IN ^{90,91}Zr*

P. Dey [a,b,†], A. Kundu[b,c], R. Palit[b], P.J. Napiorkowski[a]
E. Ideguchi[d], T. Inakura[e], F.S. Babra[b], Biswajit Das[b]
U. Garg[f], S.V. Jadhav[b], A.K. Jain[g], M. Kumar Raju[h]
Md.S.R. Laskar[b], B. Maheshwari[i], Vishal Malik[b], B.S. Naidu[b]
D. Negi[b,j], S. Pal[b], S. Sihotra[k], A. Sindhu[b], S. Thorat[b]
A.T. Vazhappilly[b]

[a]Heavy Ion Laboratory, University of Warsaw, 02-093 Warsaw, Poland
[b]Tata Institute of Fundamental Research, Mumbai 400005, India
[c]Saha Institute of Nuclear Physics, Kolkata 700064, India
[d]RCNP, Osaka University, Ibaraki, Osaka 567-0047, Japan
[e]Laboratory for Advanced Nuclear Energy, Tokyo Institute of Technology Meguro, Tokyo 152-8550, Japan
[f]University of Notre Dame, Notre Dame, IN 46556, USA
[g]Amity Institute of Nuclear Science and Technology, Amity University Noida 201313, India
[h]GITAM School of Science, GITAM University, Visakhapatnam 530045, India
[i]Faculty of Science, University of Zagreb, HR 10000, Croatia
[j]Manipal Institute of Technology, Manipal Academy of Higher Education Manipal 576104, India
[k]Panjab University, Chandigarh 160014, India

Received 29 October 2025, accepted 16 February 2026, published online 31 March 2026

A Coulomb excitation experiment has been performed with the aim of populating the 3_1^- state in ^{90}Zr at 2748 keV excitation energy with 88 MeV ^{32}S beam and particle–γ coincidence mode. A preliminary analysis has been performed to determine the electromagnetic matrix element. In a separate measurement, the octupole collective $11/2_1^-$ state in ^{91}Zr has been populated by the ^{82}Se(^{13}C, $4n$) reaction. Significantly high B(E3) strength has been determined by measuring the lifetime of this state through the electronic fast timing method.

DOI:10.5506/APhysPolBSupp.19.1-A19

* Presented at the XXXVIII Mazurian Lakes Conference on Physics, Piaski, Poland, August 31–September 6, 2025.

† Corresponding author: p.dey@uw.edu.pl

1. Introduction

The collective excitation mode and its coupling with the single-particle excitation mode in atomic nuclei remains a fundamental issue in modern nuclear structure physics [1]. At low excitation energy, the rotational and vibrational spectra of even–even nuclei provide the simplest examples of collective modes, with quadrupole and octupole excitations comprising the latter one. Due to the almost spherical ground state of nuclei near the shell closures, quadrupole collectivity is seen to be less compared to deformed nuclei. In contrast, octupole excitations in these spherical nuclei have been observed by measuring enhanced electric-octupole transition strengths, $B(\mathrm{E3})$, values [2] associated with octupole phonon states. In addition, the energies of the octupole collective vibrational modes and single-particle excitation have similar energy scales, which can favor coupling between these modes. The coupling between a valence nucleon and an octupole phonon can induce octupole collectivity in neighboring odd-A nuclei having one particle outside the even–even core by acquiring a permanent octupole deformation [3].

Recently, structural investigations up to high-spin states in nuclei in the $A \approx 90$ region with $Z \approx 40$ and $N \approx 50$ have shown their single-particle excitation that is well explained by shell-model calculations with no sign of significant collectivity [4–6]. The Zr isotopes in this mass region are mostly spherical in their ground state, and this fact is evident from their relatively high excitation energy of 2_1^+ states and small $B(\mathrm{E2}; 2_1^+ \rightarrow 0_1^+)$ values [7]. However, octupole collectivity is measured to be high enough, which aligns with the observation in many closed-shell nuclei. The existing experimental estimates of the $B(\mathrm{E3})$ values for the semimagic nucleus ^{90}Zr exhibit a wide range [2], leading to differing interpretations of the octupole collectivity in this nucleus. These $B(\mathrm{E3})$ values were measured mainly with indirect methods such as light- and heavy-ion scattering and lifetime measurements. In this regard, Coulomb excitation could be a precise technique as a model-independent probe, especially probing collective structures. The g factor measurement using only safe Coulex revealed its single particle nature, which was supported by the shell-model theory [8]. However, the calculated $B(\mathrm{E3})$ strength is underestimated by a factor of five.

Some of the latest works show an enhanced $B(\mathrm{E3})$ in odd-A nuclei in different mass regions, from the Ca to Pb isotopes. An extended description of the coupling between the valence particle/hole and the octupole phonon has been presented in Ref. [9]. Interestingly, this coupling model has successfully explained the origin of large $B(\mathrm{E3}, 19/2^- \rightarrow 13/2^+) = 40(8)$ W.u. at high-spin in ^{207}Pb as well [10]. A valence neutron occupies the $2d_{5/2}$ orbital outside $N = 50$ shell closure in ^{91}Zr and the measured lifetime of the first excited $11/2^-$ state at 2171 keV excitation energy [11] led to unrealistically high $B(\mathrm{E3}) < 1900$ W.u. In these scenarios, ^{90}Zr and ^{91}Zr isotopes serve

as an ideal testing ground for the assessment of the evolution of octupole collectivity in low-lying states across the isotopic chain by probing the spherical nature of the core and its coupling with the valence nucleon.

2. Experimental details

To explore such features, a series of new measurements has been performed on ^{90,91}Zr isotopes via different reaction mechanisms using a hybrid setup of the Indian National Gamma Array (INGA) and various ancillary detectors at the Tata Institute of Fundamental Research, India. INGA is an array of clover HPGe detectors, where the detectors are placed at different forward, backward, and 90° angles with respect to the beam direction [12].

Coulomb excitation of an isotopically enriched 1.23 mg/cm^2 thick ^{90}Zr target was performed at TIFR, Mumbai with 88 MeV ^{32}S beam provided by the TIFR-BARC Pelletron Linac Facility (PLF). The selected beam energy satisfied the required criterion for the safe Coulomb excitation with negligible nuclear interaction. An annular double-sided Si-detector (ADSSD), aligned with the beam axis, was placed upstream inside the target chamber at a distance of 2.6 cm from the target position. The ADSSD is an S3-type detector manufactured by Micron Semiconductor Ltd. which is segmented into 24 rings and 32 sectors on either side. Such segmentation provides absolute (θ_p, ϕ_p) information for the scattered particles which facilitates Doppler correction for associated γ-rays. The particle–γ coincidence was achieved by coupling this ADSSD with 16 clover HPGe detectors from INGA (see Fig. 1 (a), (b)). The time-stamped raw events from the detectors were collected in an event-by-event mode using a DDAQ system based on Pixie-16

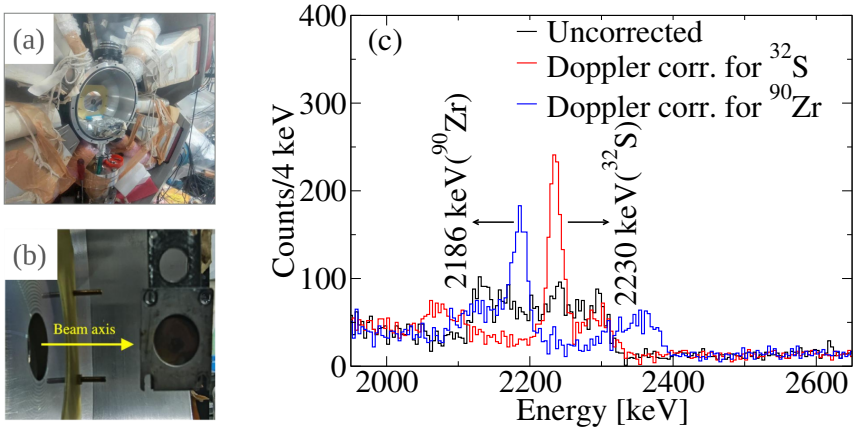

Fig. 1. (a), (b) Coincidence set-up for the Coulex experiment. (c) γ-ray energy spectra for uncorrected, Doppler corrected of ^{32}S, and ^{90}Zr from preliminary analysis. The $2_1^+ \rightarrow 0_1^+$ transition of both nuclei has been marked.

digitizing modules developed by XIA-LLC [13]. For digitizing the electronic signals, the outputs from the clover detectors and ADSSD were connected to the 12-bit 100 MHz and 14-bit 100 MHz modules, respectively. These digitized events were then sorted into energy and time histograms using a suitably modified version of "MultipARameter time-stamp-based COincidence Search program" (MARCOS) code and further analyzed using RADWARE and ROOT software packages. The detailed description and performance of this coincidence detector set-up can be found in Ref. [14].

In a separate experiment, the excited states of ^{91}Zr were populated using heavy-ion fusion–evaporation reaction with ^{197}Au backed 1 mg/cm^2 thick ^{82}Se target and 52 MeV energy ^{13}C provided by the TIFR-BARC PLF. In this experiment, 14 $LaBr_3$(Ce) detectors were coupled to the INGA to implement the electronic fast timing technique. Reference [15] discusses the exact geometry, measured and simulated performance of this hybrid array. As previously, each crystal of the clover detectors was connected to the 12-bit 100 MHz modules in a primary crate, while the faster $LaBr_3$(Ce) detectors were connected to 12-bit 250 MHz modules in a secondary crate, and both were operated together in a synchronization method. The time-stamped γ coincidence data was collected and analyzed in a similar manner as discussed earlier.

3. Data analysis and results

3.1. Coulomb excitation of ^{90}Zr

Following Coulomb scattering, the substantially high velocities β ($\equiv v/c$) of the scattered projectile and recoil target cause a significant Doppler shift in the γ energy detected by the detector. In our experiment, the coincidence measurement of the projectile-like particle at (θ_p, ϕ_p) and corresponding γ rays at $(\theta_\gamma, \phi_\gamma)$, and knowledge of β allow us to correct the γ-ray energy spectrum for the Doppler effect. In addition, a time-tagging condition between clover HPGe and ADSSD was applied to generate the final energy spectrum. Figure 1 (c) shows relevant part of the energy spectra indicating the Doppler corrected 2186 keV and 2230 keV peaks of $2_1^+ \rightarrow 0_1^+$ transition of ^{90}Zr and ^{32}S, respectively.

To determine the E3 matrix element of ^{90}Zr from Coulomb excitation data, the use of the semi-classical least squares search GOSIA code [16] is required. As there is no previous measurement of the diagonal matrix element $\langle 2_1^+ \| \mathrm{E2} \| 2_1^+ \rangle$ of ^{90}Zr, our first goal is to determine it and then use it to calculate $\langle 0_1^+ \| \mathrm{E3} \| 3_1^- \rangle$. For this calculation, the full dataset has been divided into two parts based on two different ranges of θ_p of scattered ^{32}S. Firstly, we have employed the GOSIA2 code [17], in which the details of the excitation of only 2_1^+ states of ^{32}S and ^{90}Zr have been provided. The lifetimes of

these states, and yields of the 2230 keV (for ^{32}S) and 2186 keV (for ^{90}Zr) transitions have been given as experimental data. The normalization has been done with respect to the $2_1^+ \to 0_1^+$ transition of ^{32}S by allowing to vary its $\langle 0_1^+ \| \mathrm{E2} \| 2_1^+ \rangle$ and $\langle 2_1^+ \| \mathrm{E2} \| 2_1^+ \rangle$ matrix elements. After χ^2 minimization, a starting value of $\langle 2_1^+ \| \mathrm{E2} \| 2_1^+ \rangle$ of ^{90}Zr has been obtained. In the continuation of this method, it is planned to extract a set of all possible matrix elements between relevant excited states of ^{90}Zr with the GOSIA code.

3.2. Lifetime measurements of ^{91}Zr

The predicted octupole collective $11/2_1^-$ state at 2171 keV excitation energy in the neighboring odd-A ^{91}Zr isotope is connected by several transitions (see Ref. [19]), among which the 39 keV deacying transition from the aforementioned state could not be observed due to experimental limitations in our measurements. Thus, the time difference between the 91 and 2171 keV transitions has been extracted, and then it has been corrected with the corresponding branching fraction. The timing information has been registered from the $LaBr_3$(Ce) detectors for their superior time resolution. Then the final time difference spectrum was generated by the following relation:

$$T(i) = T_{\mathrm{p}_{2171},\mathrm{p}_{91}}(i) - T_{\mathrm{p}_{2171},\mathrm{bg}_{91}}(i) - T_{\mathrm{bg}_{2171},\mathrm{p}_{91}}(i) + T_{\mathrm{bg}_{2171},\mathrm{bg}_{91}}(i)\,, \qquad (1)$$

where $T_{\mathrm{p}_{2171},\mathrm{p}_{91}}$ represents the conditional time difference spectrum obtained with the energy gates around the 2171 and 91 keV peaks, $T_{\mathrm{p}_{2171},\mathrm{bg}_{91}}$ represents the same with the energy gates around the 2171 keV peak and background near the 91 keV peak, and so on (as explained in Ref. [18]).

The time spectrum thus generated has been fitted with a convolution function of a Gaussian prompt-response function, PRF (defined by σ) and a single-component exponential decay (defined by τ) [20] as follows:

$$I(t) = I_0 \exp\left(\frac{\sigma^2}{2\tau^2} - \frac{t-\bar{t}}{\tau}\right)\left[1 - \mathrm{erf}\left(\frac{\sigma^2 - \tau\,(t-\bar{t}\,)}{\sqrt{2}\sigma\tau}\right)\right], \qquad (2)$$

where erf() corresponds to the error function, I_0 is an intensity normalization constant, and $t - \bar{t}$ is the time difference since the defined time zero. The fitted mean lifetime is $\tau^{\mathrm{expt}} = 791.6 \pm 44.1$ ps (see Fig. 2 (c)). The branching fraction for the 2171 keV γ ray, $R_B = 0.935(34)$ was calculated from the formula $R_B = I_\gamma^{2171} / \sum_{k=2171,91} I_\gamma^k (1+\alpha^k)$ (as described in Ref. [21]), using relative intensities, I_γs [22], and internal conversion coefficients, αs [23] of the decaying transitions from the $11/2_1^-$ state in ^{90}Zr. The partial γ-ray mean lifetime associated with the 2171 keV transition was then calculated from $\tau^{\mathrm{partial}} = \tau^{\mathrm{expt}}/R_B$, and was translated into reduced transition probability as $B(\mathrm{E3}; 11/2_1^- \to 5/2_1^+) = 18.5 \pm 1.2$ W.u.

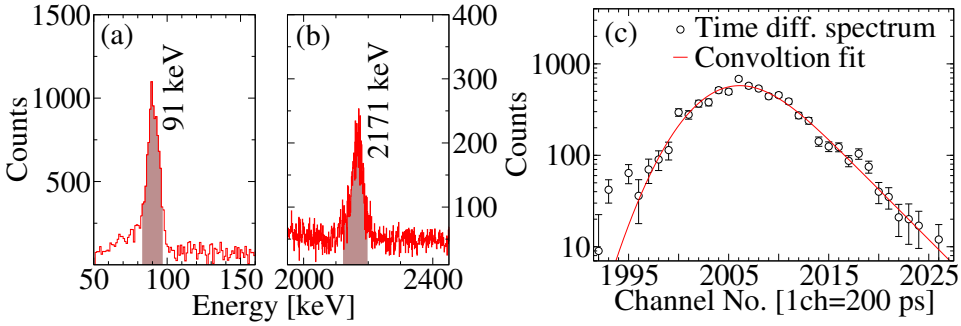

Fig. 2. (a), (b) Double-gated $LaBr_3(Ce)$ γ-ray energy spectra showing 91 keV and 2171 keV peaks of ^{91}Zr. (c) Time difference spectrum between 2171 and 91 keV transitions (see Ref. [19] for the level scheme of ^{91}Zr relevant to the present work).

The authors thank the TIFR-BARC PLF staff for the smooth operation of the accelerator. This work is supported by the Department of Atomic Energy, Government of India (Project Id. Code: 12-R&D-TFR-5.02-0200) and the Department of Science & Technology, Government of India (grant No. IR/S2/PF-03/2003-II).

REFERENCES

[1] A. Bohr, B. Mottelson, «Nuclear Structure, vol. II», *Benjamin*, 1975.
[2] T. Kibédi, R.H. Spear, *At. Data Nucl. Data Tables* **80**, 35 (2002).
[3] P. Van Isacker, M. Rejmund, *Phys. Rev. Res.* **4**, L022031 (2022).
[4] P. Dey *et al.*, *Phys. Rev. C* **105**, 044307 (2022).
[5] P. Dey *et al.*, *Phys. Rev. C* **109**, 034313 (2024).
[6] V. Malik *et al.*, *Phys. Rev. C* **111**, 024323 (2025).
[7] B. Pritychenko, M. Birch, B. Singh, M. Horoi, *At. Data Nucl. Data Tables* **107**, 1 (2016).
[8] G. Jakob *et al.*, *Phys. Lett. B* **494**, 187 (2000).
[9] S. Leoni, A. Bracco, G. Colò, B. Fornal, *Eur. Phys. J. A* **55**, 247 (2019).
[10] D. Ralet *et al.*, *Phys. Lett. B* **797**, 134797 (2019).
[11] G. Gill, R. Gill, G. Jones, *Nucl. Phys. A* **224**, 152 (1974).
[12] R. Palit, *AIP Conf. Proc.* **1336**, 573 (2011).
[13] R. Palit *et al.*, *Nucl. Instrum. Methods Phys. Res. A* **680**, 90 (2012).
[14] A. Kundu *et al.*, *Nucl. Instrum. Methods Phys. Res. A* **1069**, 169976 (2024).
[15] B. Das *et al.*, *J. Instrum. Soc. India* **51**, 44 (2021).
[16] T. Czosnyka, D. Cline, C. Wu, *Bull. Am. Phys. Soc.* **28**, 745 (1982).
[17] M. Zielińska *et al.*, *Eur. Phys. J. A* **52**, 99 (2016).

[18] E.R. Gamba, A.M. Bruce, M. Rudigier, *Nucl. Instrum. Methods Phys. Res. A* **928**, 93 (2019).

[19] Z.G. Wang *et al.*, *Phys. Rev. C* **89**, 044308 (2014).

[20] B. Olsen, L. Boström, *Nucl. Instrum. Methods* **44**, 65 (1966).

[21] F.G. Kondev, G.D. Dracoulis, T. Kibédi, *At. Data Nucl. Data Tables* **103–104**, 50 (2015).

[22] B.A. Brown, P.M.S. Lesser, D.B. Fossan, *Phys. Rev. C* **13**, 1900 (1976).

[23] BrIcc Conversion Coefficient Calculator, `https://bricc.anu.edu.au/`